Interaction with the heparin-derived binding inhibitors destabilizes galectin-3 protein structure

Paulina Sindrewicz[1], Edwin A Yates[2], Jeremy E Turnbull[2], Lu-Yun Lian[2]‡, Lu-Gang Yu[1]‡

[1]Department of Cellular and Molecular Physiology, Institute of Translational Medicine; University of Liverpool, Liverpool L69 3GE, UK

[2]Department of Biochemistry, Institute of Integrative Biology, University of Liverpool, Liverpool L69 7ZB, UK

Key words: galectin-3, heparin derivatives, differential scanning fluorimetry, isothermal titration calorimetry

‡Corresponding authors:

Prof Lu-Gang Yu, Department of Cellular and Molecular Physiology, Institute of Translational Medicine, University of Liverpool, Liverpool, L69 3GE, UK (Tel: +44 1517946820, E-mail: lgyu@liv.ac.uk)

Prof Lu-Yun Lian, Department of Biochemistry, Institute of Integrative Biology, University of Liverpool, Liverpool, L69 7ZB, UK (E-mail: lylian1@liv.ac.uk)

Abstract

The β-galactoside-binding protein, galectin-3, is extensively involved in cancer development, progression and metastasis through multiple mechanisms. Inhibition of the galectin-3-mediated actions is increasingly considered as a promising therapeutic approach for cancer treatment. Our early studies have identified several novel galectin-3 binding inhibitors from chemical modification of the anticoagulant drug heparin. These heparin-derived galectin-3 binding inhibitors, which show no anticoagulant activity and bind to the galectin-3 canonical carbohydrate-binding site, induce galectin-3 conformational changes and inhibit galectin-3-mediated cancer cell adhesion, invasion and angiogenesis *in vitro* and reduce metastasis in mice. In this study, we determined the binding affinities of these heparin-derived ligands to galectin-3 using an isothermal titration calorimetry (ITC) ligand displacement approach. Such ITC experiments showed that the 2-de-O-sulfated, N-acetylated (compound E) and 6-de-O-sulfated, N-acetylated (F) heparin-derived ligands and their ultra-low molecular weight sub-fractions (E3 and F3) bind to galectin-3 with K_D ranging from 0.96 to 1.32 mM range. Differential scanning fluorimetry analysis revealed that, in contrast to the disaccharide ligand, N-acetyl-lactosamine, which binds to the fully folded form of galectin-3 and promotes galectin-3 thermal stability, the heparin-derived ligands preferentially bind to the unfolded state of galectin-3 and cause destabilization of the galectin-3 protein structure. These results provide molecular insights into the interaction of galectin-3 with the heparin-derived ligands and explain the previously demonstrated *in vitro* and *in vivo* effects of these binding inhibitors on galectin-3-mediated cancer cell behaviours

Introduction

Galectin-3 is a unique chimera type member of the mammalian β-galactoside-binding galectin family. Galectin-3 recognises and interacts with various galactose-terminated glycans through a highly conserved carbohydrate-recognition domain (CRD) of approximately 130 amino acids arranged into a globular β-sandwich structure [1]. Galectin-3 also possesses a flexible N-terminal domain composed of a short N-terminal sequence of approximately 21 amino acids and a structurally aperiodic collagen-like tail of about 91 residues[2]. This unique N-terminal domain of galectin-3, which do not occur in other galectin members, is required for galectin-3 multimerization in the presence of ligands to confer its multivalent properties [3]. Galectin-3 is commonly overexpressed in most types of cancers [4, 5]. There is mounting evidence showing that overexpression of galectin-3 has a profound impact on cancer development, progression and metastasis via multiple mechanisms[6] These include promoting cancer cell adhesion, invasion, angiogenesis, immune suppression and metastasis by its interactions with a number of cell surface, extra- and intra-cellular proteins via protein-carbohydrate [7, 8] or protein-protein interactions [9].

The broad effects of galectin-3 on cancer progression and metastasis in wide range of cancer types have stimulated substantial interest of research laboratories and biotech companies to explore the use of galectin-3-targeting agents for cancer treatment. These agents include: Thomsen-Friedenreich antigen-mimicking molecules [10], truncated galectin-3 forms [11], peptide-based synthetic inhibitors [12, 13] as well as small carbohydrate-based inhibitors such as thiodigalactoside derivatives [14, 15] and allyl lactoside [16]. In addition, multivalent carbohydrate-based inhibitors from modified citrus pectin (MCP) and a rhamnogalacturonan-rich fragment from Ginseng pectin have also been investigated [17].

Heparin is a highly sulphated, heterogeneous polymer glycosaminoglycan with molecular weight ranging from 3 to 30 kDa. The predominant heparin disaccharide unit is composed of 2-O-sulphated iduronic acid and 6-O-sulphated, N-sulphated glucosamine, IdoA(2S)-GlcNS(6S), with some N-sulphation substituted by N-acetylation [18]. Heparin is a well-known anticoagulant and antithrombotic agent and is often used to treat cancer-associated thromboembolism in cancer patients [19]. Our recent studies have identified several chemically modified heparin derivatives as potent galectin-3 binding inhibitors [20]. These 2-de-O-sulfated, N-acetylated (compound E) and 6-de-O-sulfated, N-acetylated (compound F) heparin derivatives were produced by selective desulphation and depolymerisation from standard heparin [20]. These chemically modified heparin derivatives and their ultra-low molecular weight sub-fractions (<3 kDa) (E3 and F3) show no anticoagulant activity, bind to the galectin-3 CRD domain and inhibit galectin-3-mediated cancer cell adhesion, invasion, angiogenesis *in vitro* and reduces metastasis *in vivo* [20]. These heparin-derived galectin-3 binding inhibitors are therefore good candidates to be developed as galectin-3-targeting therapeutic agents for cancer treatment.

In this study, we determined the binding affinities of these heparin-derived inhibitors to galectin-3 using an isothermal titration calorimetry (ITC) competition (ligand displacement) approach. We also investigated the binding characteristics of galectin-3 with these novel binding inhibitors by differential scanning fluorimetry (DSF) and compared their binding with a common disaccharide binding ligand, N-acetyl-D-lactosamine (LacNAc). Our investigation revealed some unusual features of interactions of these heparin-derived ligands with galectin-3.

Materials and methods

Production of chemically modified heparin derivatives

The two chemically modified heparin derivatives, E and F and their ultra-low molecular weight fractions, E3 and F3, were prepared as previously described [18, 20].

Production of full length and C-terminally truncated recombinant human galectin-3

The full-length human galectin-3 (Gal-3, residues 1-250) and a C-terminally truncated galectin-3 form Gal-3C (residues 115-250) were produced in *E.coli* as previously described [8, 20].

ITC ligand displacement analysis

All experiments were performed at 25^0C using an MICROCAL iTC200 Microcalorimeter (Malvern) with 200 µl cell capacity and 40 µl injection syringe volume. For the reference run, Gal-3 at 100 µM in the sample cell was titrated with 2 mM LacNAc. To determine the K_D values for the four heparin-derived ligands, galectin-3 at 100 µM was incubated for 20 minutes with three different concentrations of the heparin derivatives (0.5, 1 and 2 mM) before 2 mM LacNAc was injected into the Gal-3-heparin derivative complex solution. All experiments were performed in PBS pH 7.4. LacNAc titration into buffer alone and heparin derivative solutions as well as buffer titration into galectin-3 alone were performed in control. All the control experiments exhibited undetectable heat exchange confirming appropriate buffer match and lack of dilution effect. All the ligands were tested at several concentrations to obtain a range of K_D^{app} values. K_D values for galectin-3-ligand interactions obtained by displacement of LacNAc were determined using the equation:

$\mathbf{K_D^{app} = K_D + [[K_D / Ki][L]]}$ where: $\boldsymbol{K_D^{app}}$ is the apparent K_D for the galectin-3 and LacNAc interactions in the presence of a heparin derivative, $\boldsymbol{K_D}$ is the K_D value for galectin-3-LacNAc

interactions in the absence of a heparin derivative, K_i is inhibitory K_D which represents the true K_D value for the galectin-3-heparin derivative interactions and $[L]$ is the concentration of the heparin derivative. K_i is calculated from K_D^{app} determined at different heparin-derivatives concentrations [L] [21]. Two independent ITC runs were carried out for each ligand.

DSF analysis

Galectin-3 or Gal-3C at 10 or 20 µM was mixed with LacNAc or heparin derivative at several different concentrations. SYPRO Orange (1:400 dilution) was added and the reaction volume was topped up with buffer to a total of 75 µl. Twenty-five µl reactions were then transferred in triplicates into the wells of a MicroAmp Fast Optical 96-well reaction plate. The plate was inserted into StepOne Real Time qPCR. The "Melt Curve" option was selected and the thermal denaturation was analysed with the following settings: initial temperature equilibration step at 25^0C for 1 min, followed by gradual increase in the temperature by 0.3^0C up to 95^0C. LacNAc and the heparin derivatives were also tested without the presence of galectin-3 to confirm the lack of interactions between the ligands and the dye. The data was analysed using TmTool v1.0 to derive melting temperature and Boltzmann constants. Three independent experiments, each in triplicate, were carried out for each ligand.

Results

Analysis of galectin-3 interactions with the heparin-derived ligands using ITC ligand displacement

ITC is the gold standard method for studying protein-ligand interactions. It measures the heat generated or absorbed during molecular interactions. Our early study indicated that the interaction between galectin-3 and the heparin-derived ligand F3 are relatively weak [22], hence making it difficult to achieve the high concentrations of both the ligand and the proteins required to obtain a reliable binding isotherm by direct ITC analysis. To obtain more accurate measurements of galectin-3 interaction with all the heparin derived binding ligands, we employed an ITC ligand displacement approach in this study and analysed galectin-3 interaction with each of these polysaccharide-based galectin-3 binding ligands.

The disaccharide LacNAc is a well-known galectin-3 ligand. LacNAc and the heparin-derived ligands all bind to the galectin-3 canonical carbohydrate-binding site within the galectin-3 CRD but more galectin-3 amino acid residues have shown to be involved in interaction with the heparin derivative ligands than with LacNAc in our early study [20]. In this ligand displacement analysis, LacNAc was used as a reference ligand to galectin-3 for binding competition with the heparin-derived inhibitors. Galectin-3 at 100 µM was mixed and incubated without or with heparin derivative E, F, E3 or F3 at 0 µM, 500 µM, 1 mM and 2 mM before the Gal-3-heparin derivative solution was titrated with 2 mM LacNAc. LacNAc alone binds to galectin-3 with a K_D of ~ 26.3 ± 0.5 µM (Figs 1 and 2), which is similar to the affinities reported previously using ITC and other methods [23-26]. The presence of each of the four heparin-derived ligands caused a decrease in LacNAc binding affinity to galectin-3 in a dose-dependent manner as well as clear reduction in the heat change upon binding (Fig 1A and C, Fig 2A and C). The estimated K_D values of LacNAc binding to galectin-3

increased from 26.3 to 64.4 ± 4.0 μM with increasing concentrations of the heparin derivative E from 0 to 2 mM (Fig 1A), and from 26.3 to 66.9 ± 7.9 μM with increasing concentrations of F (Fig 1C). Overlays of the ITC titration traces of galectin-3-LacNAc interactions in the presence of E or F (Fig 1B and D) showed changes in the shape of the fitting curves with increasing E and F concentrations, indicating weakening of LacNAc-galectin-3 interactions and thus, a competition between LacNAc and the heparin-derived ligands. Analysis of the K_D^{app} values obtained from the presence of different concentrations of heparin derivatives against the derivative concentrations showed binding of E (Fig 1B) and F (Fig 1D) to galectin-3 with K_D of 1.32 mM and 1.25 mM, respectively.

The presence of the ultra-low molecular weight sub-fractions of the heparin derivatives E3 and F3 showed stronger competition with LacNAc for binding to galectin-3 in comparison to the unfractionated E and F (Fig 2A and C). The K_D values of LacNAc binding to galectin-3 increased from 26.3 to 67.4 ± 3.5 μM with E3 and from 26.3 to 77.3 ± 8.5 μM in the presence of F3 with increasing heparin derivative concentrations. Again, overlays of the ITC traces of LacNAc titrations into galectin-3-heparin derivatives complex solutions (Fig 2B and D) show clear shallowing of the binding curves, indicating a weaker LacNAc binding to the protein. Analysis of the K_D^{app} values, obtained in the presence of different concentrations of E3 and F3, against the derivative concentrations allowed determination of the binding affinities for E3 (Fig 1B) and F3 (Fig 1D) to be 1.15 mM and 0.96 mM, respectively. The stronger competition with LacNAc exhibited by E3 and F3 for binding to galectin-3 than their unfractionated counterparts E and F, is in good agreement with the stronger effect of E3 and F3, than E and F, on galectin-3-mediated cell adhesion and metastasis in mice observed in our previous study [20].

Analysis of galectin-3 interactions with the heparin-derived inhibitors by DSF

Differential Scanning Fluorimetry monitors the unfolding transition of proteins in response to change of temperature and can provide insight into the effect of ligand binding on the thermal stability of a protein.

In these experiments, we first determined the thermal stability of Gal-3C (20 µM) in the presence of different concentrations of LacNAc. Gal-3C alone was observed to have a melting temperature (T_m) of 60.4^{0}C (Fig 3A). Upon the addition of increasing concentrations of LacNAc from 0 to 400 µM, the unfolding curves of Gal-3C were, as expected, shifted to higher temperatures (Fig 3A). The change in the melting temperature from 60.4^{0}C to 61.9^{0}C in the presence of 400 µM LacNAc (ΔT_m = 1.5^{0}C) (Fig 3F), indicates an increase in the thermal stability of galectin-3C upon LacNAc binding.

Gal-3C thermodenaturation was assessed in the presence of the heparin-derived ligands at several different E and F concentrations ranging from 0 to 200 µg/ml, and E3 and F3 from 0 and 100 µM (equivalent to approximately 0-300 µg/ml, assuming their MW= 3000 Da). The presence of each of the four heparin derivatives showed an opposite effect to LacNAc on Gal-3C thermal stability. In contrast to LacNAc, binding of the heparin derivatives decreased Gal-3C melting temperature in a heparin derivative dose-dependent manner (Fig 3B-E). The greatest change in Gal-3C T_m among these polysaccharides was caused by F3 (ΔT_m of 2.1 ^{0}C) and followed by F (ΔT_m of 2.0^{0}C) (Fig 3F and G). E and E3, both caused a reduction in Gal-3C melting temperatures by 1.5 ^{0}C (Fig 3F and G). These indicate that in contrast to galectin-3C stabilisation upon LacNAc binding, interactions of the heparin derivatives with galectin-3 destabilize galectin-3C structure.

To test whether the destabilization effect of the heparin-derived ligands was not specific to the C-terminal domain of galectin-3, we analyzed the impact of those inhibitors on thermal stability of the full-length galectin-3. In the absence of a ligand, the full-length galectin-3 showed a slightly lower melting temperature (T_m=58.8^{0}C) than the truncated form of Gal-3C (Fig 3A and 4A). This reduction in the melting temperature is likely due to the presence of the unstructured, collagen-like N-terminal domain in the full-length galectin-3. Similar to Gal-3C, the presence of LacNAc induced a dose-dependent thermal stabilization of the full-length galectin-3 structure indicated by the rise in the T_m. At 800 μM LacNAc binding enhanced the galectin-3 melting temperature by 1.9^{0}C (Fig 4A and D). The presence of the heparin-derived ligands E3 (Fig 4B) and F3 (Fig 4C) again, produced opposite effect to LacNAc and induced a decrease in galectin-3 thermal stability with increasing ligand concentrations. At the highest tested concentration of 333 μM (approximately 1 mg/ml), E3 and F3 caused a reduction in galectin-3 T_m by 1.4 ^{0}C and 1.5 ^{0}C, respectively.

Discussion

In this study, an ITC-based ligand displacement analysis revealed the binding affinities of the heparin-derived inhibitors to galectin-3 at low mM range. In contrast to the binding of disaccharide ligand LacNAc to galectin-3, which enhances galectin-3 structure stability, binding of the heparin-derived ligands to galectin-3 interestingly showed thermal destabilization of the galectin-3 native structure.

It was found in this study that the ultra-low molecular weight sub-fractions E3 and F3 bound galectin-3 with higher affinities than their unfractionated counterparts E and F. This agrees with the stronger effect of E3 and F3, than E and F, on inhibition of galectin-3-mediated activities *in vitro* and *in vivo* shown in our previous study [20]. None of the heparin-derived inhibitors contains the canonical galectin-3 binding monosaccharide moiety, galactose. Their low binding affinities to galectin-3 revealed in this study are, therefore, not very surprising. However, these heparin-derived inhibitors are complex long polysaccharides and each can potentially bind to multiple galectin-3 molecules. Thus, although, binding of these heparin derivatives to galectin-3 is not very strong, the impact of their binding on galectin-3-mediated actions could still be very significant *in vivo*, due in part to their abilities to provide a scaffold for binding multiple galectin-3 molecules. The significant effect of these heparin derivatives on inhibition of galectin-3-mediated cancer cell adhesion, invasion, angiogenesis and metastasis observed with cancer cells and in mice indeed supports this.

DFS analysis in this study showed that binding of these heparin-derived inhibitors to galectin-3 induces destabilization of the galectin-3 protein structure, which is different to the galectin-3 binding by the disaccharide ligand LacNAc which enhances galectin-3 thermal stability. DSF measurements are based on the principle that ligand binding to a protein alters

the protein's thermal stability and leads to a shift in the midpoint of the unfolding transition of the protein. In general, ligand binding causes an increase in the protein thermal stability shown by a rise in the protein melting temperature with increasing ligand concentrations. Such ligands which bind to the native state of the protein and stabilise the protein structure are called N-binders or upshifters. Some ligands preferentially bind to the unfolded state of a protein, cause a destabilisation and promote unfolding. This class of ligands, which reduce the protein melting temperature in DFS measurements, is called U-binders or downshifters [27]. In this study, LacNAc binding to galectin-3 showed a classical binding pattern of N-binders which increased protein melting temperature with increasing LacNAc concentration. In contrast, the heparin-derived inhibitors showed the classical behavior of U-binders that reduce the protein melting temperature with increasing ligand concentrations. This indicates that the heparin-derived ligands preferentially bind to the partially unfolded state of galectin-3 and induce thermal destabilization of the galectin-3 structure. The effect of these heparin derived ligands on galectin-3 structure destabilization concurs well with our early discovery that binding of these heparin-derived inhibitors to galectin-3 induces galectin-3 conformation changes as assessed by synchrotron radiation circular dichroism [20].

In this study, an ITC competition (ligand displacement) approach was used to determine the dissociation constants of the heparin-derived inhibitors with galectin-3. While direct ITC measurements can reliably characterise protein-ligand interactions with binding affinities >1 nM and <100 μM [28], it often faces challenges in accurate determination of high affinity ligand binding with K_D in picomolar/low nanomolar range as well as of weak ligand binding with K_D in mM range. ITC competition approach has been previously used to determine dissociation constants of very strong binding ligands [28, 29], in which the association constant (K_A) for the high affinity ligands is artificially lowered to a measurable level by

introduction of a weaker competitive ligand. In this study, the ITC competition experimental mode was successfully applied to measure the dissociation constants of low-affinity polysaccharide ligands. This provides support to the effectiveness of using ITC ligand displacement approach in determining weak binding ligands which so far has only been reported in very few studies [30, 31].

In conclusion, the binding affinity of the heparin-derived inhibitors to galectin-3 is in the low mM range. In contrast to LacNAc, which binds to the fully-folded state of galectin-3 and enhances galectin-3 protein stability, the heparin-derived inhibitors preferentially bind to the partially unfolded state of galectin-3 and destabilize the protein structure. These discoveries provide insight into the molecular interaction of galectin-3 with the heparin derivatives. The influence of these novel binding ligands on galectin-3 protein stability revealed in this study may itself be an independent mechanism of their inhibitory effect on galectin-3-mediated cancer cell behaviours shown *in vitro* and *in vivo* in our previous studies. The information from this study may be useful in future development of these novel binding inhibitors as galectin-3-targeted therapeutic agents in cancer as well as other galectin-3-associated human diseases.

Acknowledgements: This study was supported by a Medical Research Council Industry Case Studentship (MR/L014327/1)

Conflicts of interest: EAY, JET and LGY are named as inventors on a patent covering the use of the heparin derivative inhibitors as anti-metastatic agents. JET and EAY hold shares in IntelliHep Ltd which currently holds an option to licence this patent. The other authors declare no conflict of interest

Abbreviations

BSA, bovine serum albumin; CRD, carbohydrate-recognition domain; Gal-3C, C-terminal domain of galectin-3; DSF, Differential Scanning Fluorimetry; ITC, Isothermal Titration Calorimetry; LacNAc, N-acetyl-lactosamine; T_m, melting temperature

Figure legends

Figure 1. Analysis of galectin-3 interactions with heparin-derived ligands E and F by ITC ligand displacement. Galectin-3 (100 µM) was mixed with 0, 0.5, 1.0 and 2.0 mM E **(A)** or F **(C)** before titration with 2 mM LacNAc. The integrated ITC data was fitted to a *One set of sites* interaction model and the dissociation constants (K_D) were determined. The K_D^{app} was plotted against heparin derivative concentration and the K_D values for galectin-3 interactions with E **(B)** and F **(D)** were calculated using the equation described in the Methods section. Data are expressed as mean ± SD from two independent experiments.

Figure 2. Analysis of galectin-3 interactions with heparin-derived ligands E3 and F3 by ITC ligand displacement. Galectin-3 (100 µM) was mixed with 0, 0.5, 1.0 and 2.0 mM E3 **(A)** or F3 **(C)** before titration with 2 mM LacNAc. The integrated ITC data was fitted to a *One set of sites* interaction model and the dissociation constants (K_D) were determined. The K_D^{app} was plotted against heparin derivative concentration and the K_D values for galectin-3 interactions with E3 **(B)** and F3 **(D)** were calculated using the equation described in the Methods section. Data are expressed as mean ± SD from two independent experiments.

Figure 3. Investigation of Gal-3C interaction with LacNAc and the heparin-derived ligands by DSF.

Gal-3C thermodenaturation curves in the presence of LacNAc **(A)**, E **(B)**, F **(C)**, E3 **(D)** and F3 **(E)** at different concentrations were analysed by DSF. A shift of the melting curves to a higher temperature with increasing LacNAc concentrations and shifts to lower temperatures with increasing heparin derivative concentrations were observed. Panels F and G show the magnitude of melting temperature changes for each of the conditions indicated. Data were obtained from three independent experiments, each in triplicates.

Figure 4. **Investigation of full-length galectin-3 interactions with LacNAc and the heparin-derived ligands by DSF**.

Galectin-3 thermodenaturation curves in the presence of LacNAc **(A)**, E3 **(B)** and F3 **(C)** at different concentrations were determined by DSF. A shift of the melting curves to a higher temperature with increasing LacNAc concentrations and shifts to lower temperature with increased heparin derivative concentrations were observed. Panel D shows the magnitude of melting temperature changes for each of the conditions indicated. Data were obtained from three independent experiments, each in triplicates.

References

[1] S.H. Barondes, D.N.W. Cooper, M.A. Gitt, H. Leffler, GALECTINS - STRUCTURE AND FUNCTION OF A LARGE FAMILY OF ANIMAL LECTINS, J Biol Chem, 269 (1994) 20807-20810.
[2] A. Flores-Ibarra, S. Vértesy, F.J. Medrano, H.-J. Gabius, A. Romero, Crystallization of a human galectin-3 variant with two ordered segments in the shortened N-terminal tail, Sci Rep, 8 (2018).
[3] H.C. Gong, Y. Honjo, P. Nangia-Makker, V. Hogan, N. Mazurak, R.S. Bresalier, A. Raz, The NH2 terminus of galectin-3 governs cellular compartmentalization and functions in cancer cells, Cancer Res, 59 (1999) 6239-6245.
[4] F.-T. Liu, G.A. Rabinovich, Galectins as modulators of tumour progression., Nat Rev Cancer, 5 (2005) 29-41.
[5] L. Johannes, R. Jacob, H. Leffler, Galectins at a glance, J Cell Sci, 131 (2018) jcs208884.
[6] A.U. Newlaczyl, L.G. Yu, Galectin-3: A-jack-of-all-trades in cancer, Cancer Lett, 313 (2011) 123-128.
[7] L.-G. Yu, N. Andrews, Q. Zhao, D. McKean, J.F. Williams, L.J. Connor, O.V. Gerasimenko, J. Hilkens, J. Hirabayashi, K. Kasai, J.M. Rhodes, Galectin-3 interaction with Thomsen-Friedenreich disaccharide on cancer-associated MUC1 causes increased cancer cell endothelial adhesion, J Biol Chem, 282 (2007) 773-781.
[8] F. Colomb, W. Wang, D. Simpson, M. Zafar, R. Beynon, J.M. Rhodes, L.G. Yu, Galectin-3 interacts with the cell-surface glycoprotein CD146 (MCAM, MUC18) and induces secretion of metastasis-promoting cytokines from vascular endothelial cells, J Biol Chem, 292 (2017) 8381-8389.
[9] F.T. Liu, R.J. Patterson, J.L. Wang, Intracellular functions of galectins, BBA, 1572 (2002) 263-273.
[10] V.V. Glinsky, G. Kiriakova, O.V. Glinskii, V.V. Mossine, T.P. Mawhinney, J.R. Turk, A.B. Glinskii, V.H. Huxley, J.E. Price, G.V. Glinsky, Synthetic galectin-3 inhibitor increases metastatic cancer cell sensitivity to taxol-induced apoptosis in vitro and in vivo, Neoplasia, 11 (2009) 901-909.
[11] C.M. John, H. Leffler, B. Kahl-Knutsson, I. Svensson, G.a. Jarvis, Truncated galectin-3 inhibits tumor growth and metastasis in orthotopic nude mouse model of human breast cancer, Clin Cancer Res, 9 (2003) 2374-2383.
[12] J. Zou, V.V. Glinsky, L.a. Landon, L. Matthews, S.L. Deutscher, Peptides specific to the galectin-3 carbohydrate recognition domain inhibit metastasis-associated cancer cell adhesion., Carcinogenesis, 26 (2005) 309-318.
[13] A. Moise, S. André, F. Eggers, M. Krzeminski, M. Przybylski, H.-J. Gabius, Toward Bioinspired Galectin Mimetics: Identification of Ligand-Contacting Peptides by Proteolytic-Excision Mass Spectrometry, J Am Chem Soc, 133 (2011) 14844-14847.
[14] C.T. Oberg, H. Leffler, U.J. Nilsson, Inhibition of galectins with small molecules, Chimia, 65 (2011) 18-23.
[15] B.A. Salameh, I. Cumpstey, A. Sundin, H. Leffler, U.J. Nilsson, 1H-1,2,3-triazol-1-yl thiodigalactoside derivatives as high affinity galectin-3 inhibitors, Bioorg Med Chem, 18 (2010) 5367-5378.
[16] I. Iurisci, A. Cumashi, A.a. Sherman, Y.E. Tsvetkov, N. Tinari, E. Piccolo, M. D'Egidio, V. Adamo, C. Natoli, G.a. Rabinovich, S. Iacobelli, N.E. Nifantiev, Synthetic inhibitors of galectin-1 and -3 selectively modulate homotypic cell aggregation and tumor cell apoptosis, Anticancer Res, 29 (2009) 403-410.
[17] H. Blanchard, X. Yu, P.M. Collins, K. Bum-erdene, Galectin-3 inhibitors : a patent review (2008 -- present), (2014) 1053-1065.
[18] E.A. Yates, F. Santini, M. Guerrini, A. Naggi, G. Torri, B. Casu, H-1 and C-13 NMR spectral assignments of the major sequences of twelve systematically modified heparin derivatives, Carbohydr Res, 294 (1996) 15-27.
[19] L. Borsig, Heparin as an inhibitor of cancer progression, Prog Mol Biol Transl Sci, 93 (2010) 335-349.
[20] C.A. Duckworth, S.E. Guimond, P. Sindrewicz, A.J. Hughes, N.S. French, L.-y. Lian, E.A. Yates, D.M. Pritchard, J.M. Rhodes, J.E. Turnbull, L.-g. Yu, Chemically modified, non-anticoagulant heparin

derivatives are potent galectin-3 binding inhibitors and inhibit circulating galectin-3-promoted metastasis, Oncotarget, 6 (2015) 23671-23687.
[21] B.W. Sigurskjold, Exact analysis of competition ligand binding by displacement isothermal titration calorimetry, Anal Biochem, 277 (2000) 260-266.
[22] P. Sindrewicz, X. Li, E.A. Yates, J.E. Turnbull, L.Y. Lian, L.G. Yu, Intrinsic tryptophan fluorescence spectroscopy reliably determines galectin-ligand interactions, Sci Rep, 9 (2019) 11851.
[23] T.J. Hsieh, H.Y. Lin, Z. Tu, B.S. Huang, S.C. Wu, C.H. Lin, Structural basis underlying the binding preference of human galectins-1, -3 and -7 for Galβ1-3/4GlcNAc, PLoS ONE, (2015).
[24] M.C. Rodriguez, S. Yegorova, J.P. Pitteloud, A.E. Chavaroche, S. André, A. Ardá, D. Minond, J. Jiménez-Barbero, H.J. Gabius, M. Cudic, Thermodynamic Switch in Binding of Adhesion/Growth Regulatory Human Galectin-3 to Tumor-Associated TF Antigen (CD176) and MUC1 Glycopeptides, Biochemistry, 54 (2015) 4462-4474.
[25] K. Saraboji, M. Håkansson, S. Genheden, C. Diehl, J. Qvist, U. Weininger, U.J. Nilsson, H. Leffler, U. Ryde, M. Akke, D.T. Logan, M. Hakansson, S. Genheden, C. Diehl, J. Qvist, U. Weininger, U.J. Nilsson, H. Leffler, U. Ryde, M. Akke, D.T. Logan, The Carbohydrate-Binding Site in Galectin-3 Is Preorganized To Recognize a Sugarlike Framework of Oxygens: Ultra-High-Resolution Structures and Water Dynamics, Biochemistry, 51 (2012) 296-306.
[26] C. Diehl, O. Engström, T. Delaine, M. Håkansson, S. Genheden, K. Modig, H. Leffler, U. Ryde, U.J. Nilsson, M. Akke, Protein flexibility and conformational entropy in ligand design targeting the carbohydrate recognition domain of galectin-3, J Am Chem Soc, (2010).
[27] P. Cimmperman, L. Baranauskiene, S. Jachimoviciute, J. Jachno, J. Torresan, V. Michailoviene, J. Matuliene, J. Sereikaite, V. Bumelis, D. Matulis, A quantitative model of thermal stabilization and destabilization of proteins by ligands, Biophys J, 95 (2008) 3222-3231.
[28] G. Krainer, S. Keller, Single-experiment displacement assay for quantifying high-affinity binding by isothermal titration calorimetry, Methods, 76 (2015) 116-123.
[29] A. Velazquez-Campoy, E. Freire, Isothermal titration calorimetry to determine association constants for high-affinity ligands, Nat Protoc, 1 (2006) 186-191.
[30] E. Ruhmann, M. Betz, M. Fricke, A. Heine, M. Schafer, G. Klebe, Thermodynamic signatures of fragment binding: Validation of direct versus displacement ITC titrations, Biochim Biophys Acta, 1850 (2015) 647-656.
[31] Y.L. Zhang, Z.Y. Zhang, Low-affinity binding determined by titration calorimetry using a high-affinity coupling ligand: a thermodynamic study of ligand binding to protein tyrosine phosphatase 1B, Anal Biochem, 261 (1998) 139-148.

Fig 1

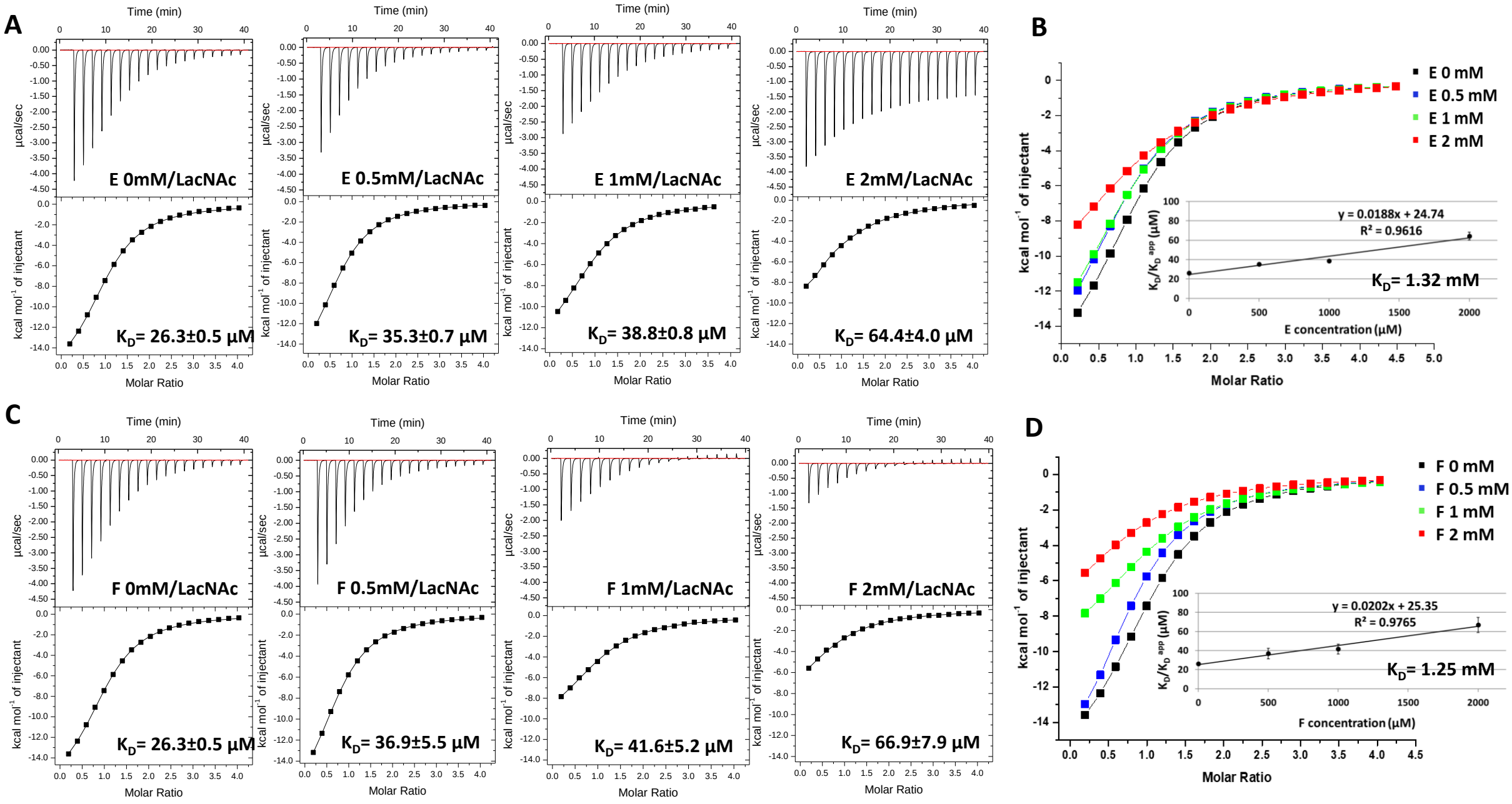
A
Time (min)
µcal/sec
kcal mol-1 of injectant
Molar Ratio
E 0mM/LacNAc
KD= 26.3±0.5 µM
E 0.5mM/LacNAc
KD= 35.3±0.7 µM
E 1mM/LacNAc
KD= 38.8±0.8 µM
E 2mM/LacNAc
KD= 64.4±4.0 µM
B
E 0 mM
E 0.5 mM
E 1 mM
E 2 mM
y = 0.0188x + 24.74
R² = 0.9616
KD= 1.32 mM
KD/KD app (µM)
E concentration (µM)
C
F 0mM/LacNAc
KD= 26.3±0.5 µM
F 0.5mM/LacNAc
KD= 36.9±5.5 µM
F 1mM/LacNAc
KD= 41.6±5.2 µM
F 2mM/LacNAc
KD= 66.9±7.9 µM
D
F 0 mM
F 0.5 mM
F 1 mM
F 2 mM
y = 0.0202x + 25.35
R² = 0.9765
KD= 1.25 mM
F concentration (µM)

Fig 2

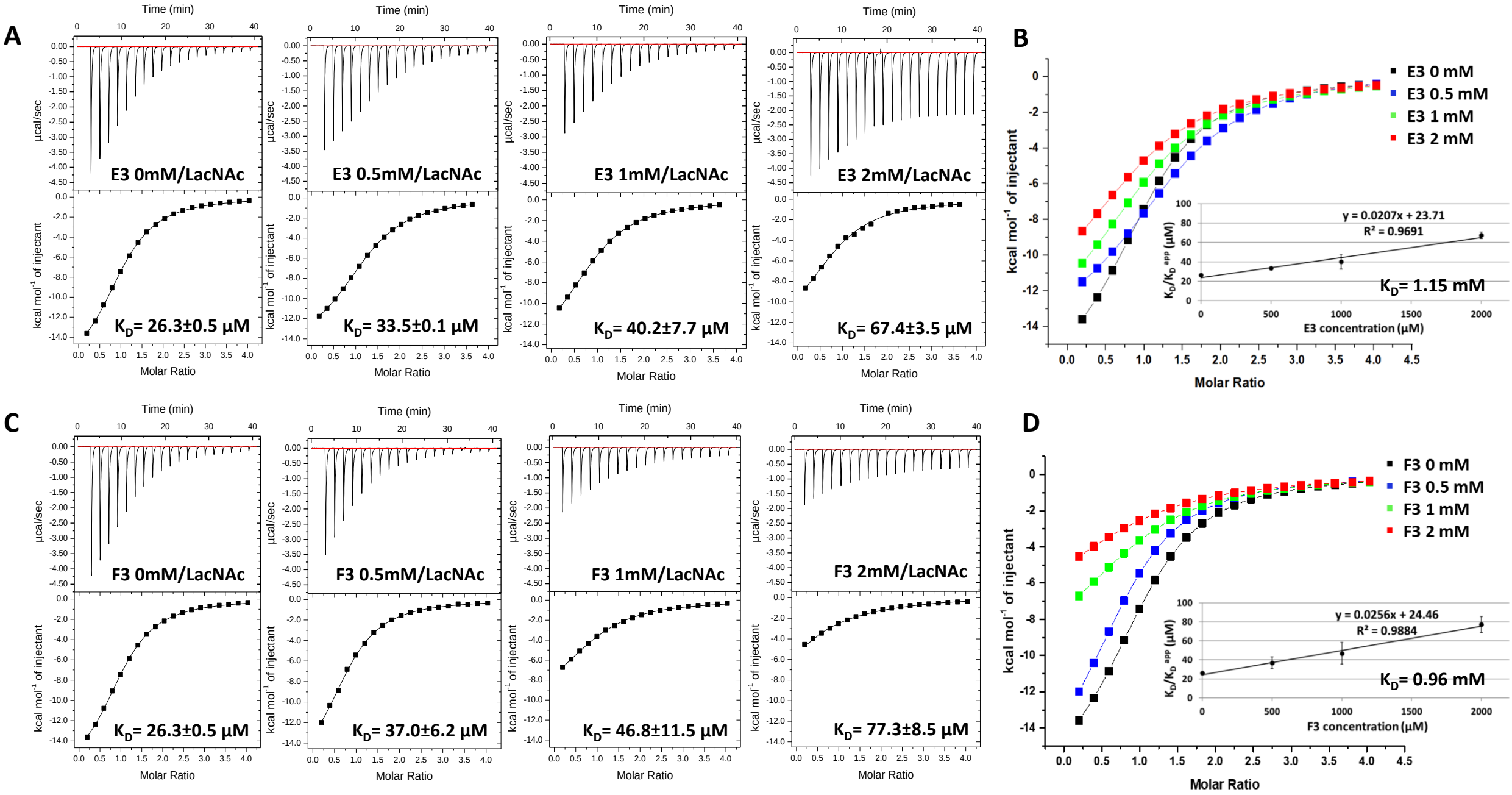
A
Time (min)
µcal/sec
kcal mol-1 of injectant
Molar Ratio
E3 0mM/LacNAc
KD= 26.3±0.5 µM
E3 0.5mM/LacNAc
KD= 33.5±0.1 µM
E3 1mM/LacNAc
KD= 40.2±7.7 µM
E3 2mM/LacNAc
KD= 67.4±3.5 µM
B
E3 0 mM
E3 0.5 mM
E3 1 mM
E3 2 mM
y = 0.0207x + 23.71
R² = 0.9691
KD/KD app (µM)
E3 concentration (µM)
KD= 1.15 mM
C
F3 0mM/LacNAc
KD= 26.3±0.5 µM
F3 0.5mM/LacNAc
KD= 37.0±6.2 µM
F3 1mM/LacNAc
KD= 46.8±11.5 µM
F3 2mM/LacNAc
KD= 77.3±8.5 µM
D
F3 0 mM
F3 0.5 mM
F3 1 mM
F3 2 mM
y = 0.0256x + 24.46
R² = 0.9884
F3 concentration (µM)
KD= 0.96 mM

Fig 3

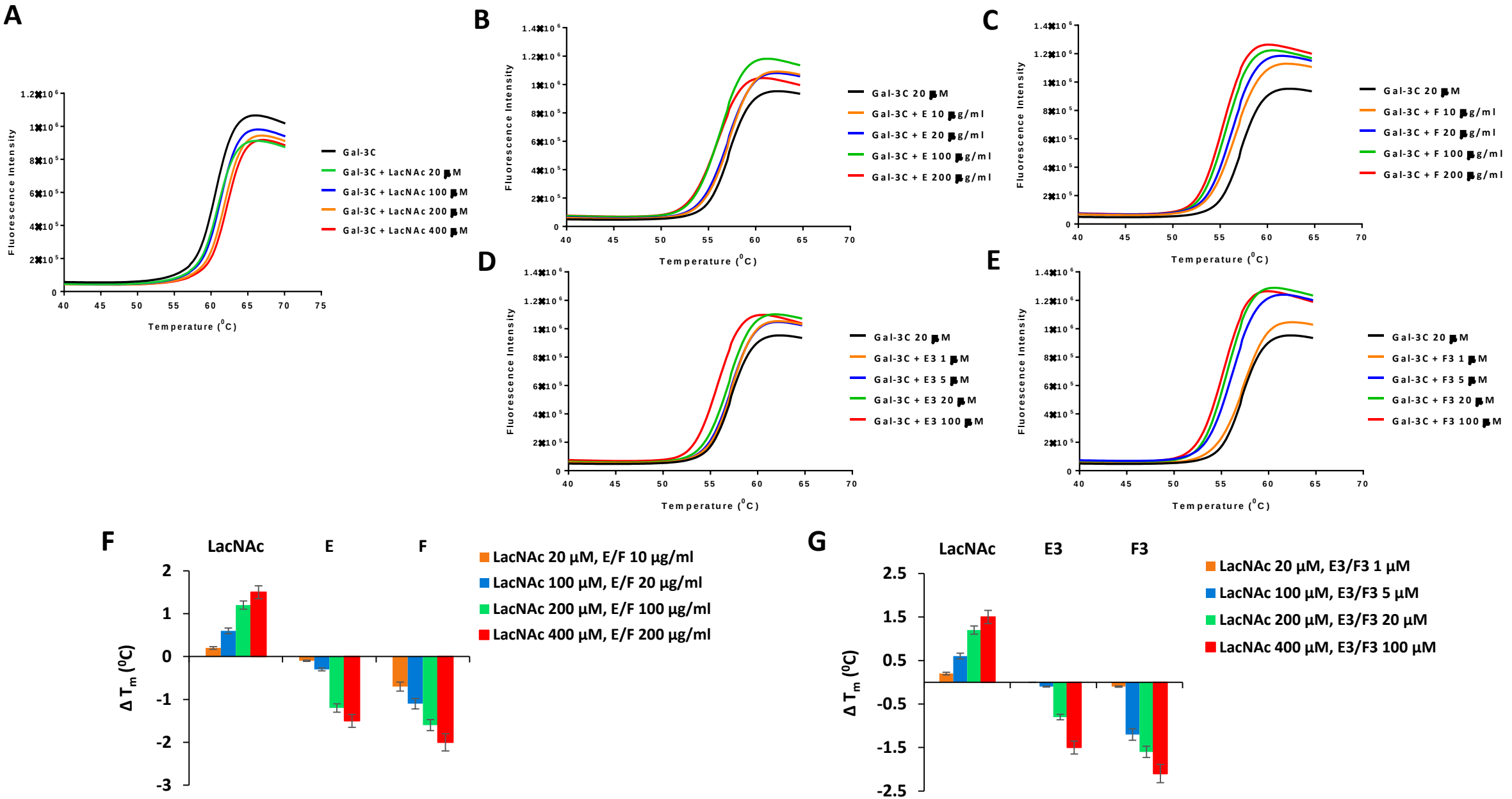
A
Fluorescence Intensity
Temperature (°C)
Gal-3C
Gal-3C + LacNAc 20 µM
Gal-3C + LacNAc 100 µM
Gal-3C + LacNAc 200 µM
Gal-3C + LacNAc 400 µM
B
Gal-3C 20 µM
Gal-3C + E 10 µg/ml
Gal-3C + E 20 µg/ml
Gal-3C + E 100 µg/ml
Gal-3C + E 200 µg/ml
C
Gal-3C 20 µM
Gal-3C + F 10 µg/ml
Gal-3C + F 20 µg/ml
Gal-3C + F 100 µg/ml
Gal-3C + F 200 µg/ml
D
Gal-3C 20 µM
Gal-3C + E3 1 µM
Gal-3C + E3 5 µM
Gal-3C + E3 20 µM
Gal-3C + E3 100 µM
E
Gal-3C 20 µM
Gal-3C + F3 1 µM
Gal-3C + F3 5 µM
Gal-3C + F3 20 µM
Gal-3C + F3 100 µM
F
LacNAc
E
F
Δ Tm (°C)
LacNAc 20 µM, E/F 10 µg/ml
LacNAc 100 µM, E/F 20 µg/ml
LacNAc 200 µM, E/F 100 µg/ml
LacNAc 400 µM, E/F 200 µg/ml
G
LacNAc
E3
F3
Δ Tm (°C)
LacNAc 20 µM, E3/F3 1 µM
LacNAc 100 µM, E3/F3 5 µM
LacNAc 200 µM, E3/F3 20 µM
LacNAc 400 µM, E3/F3 100 µM

Fig 4

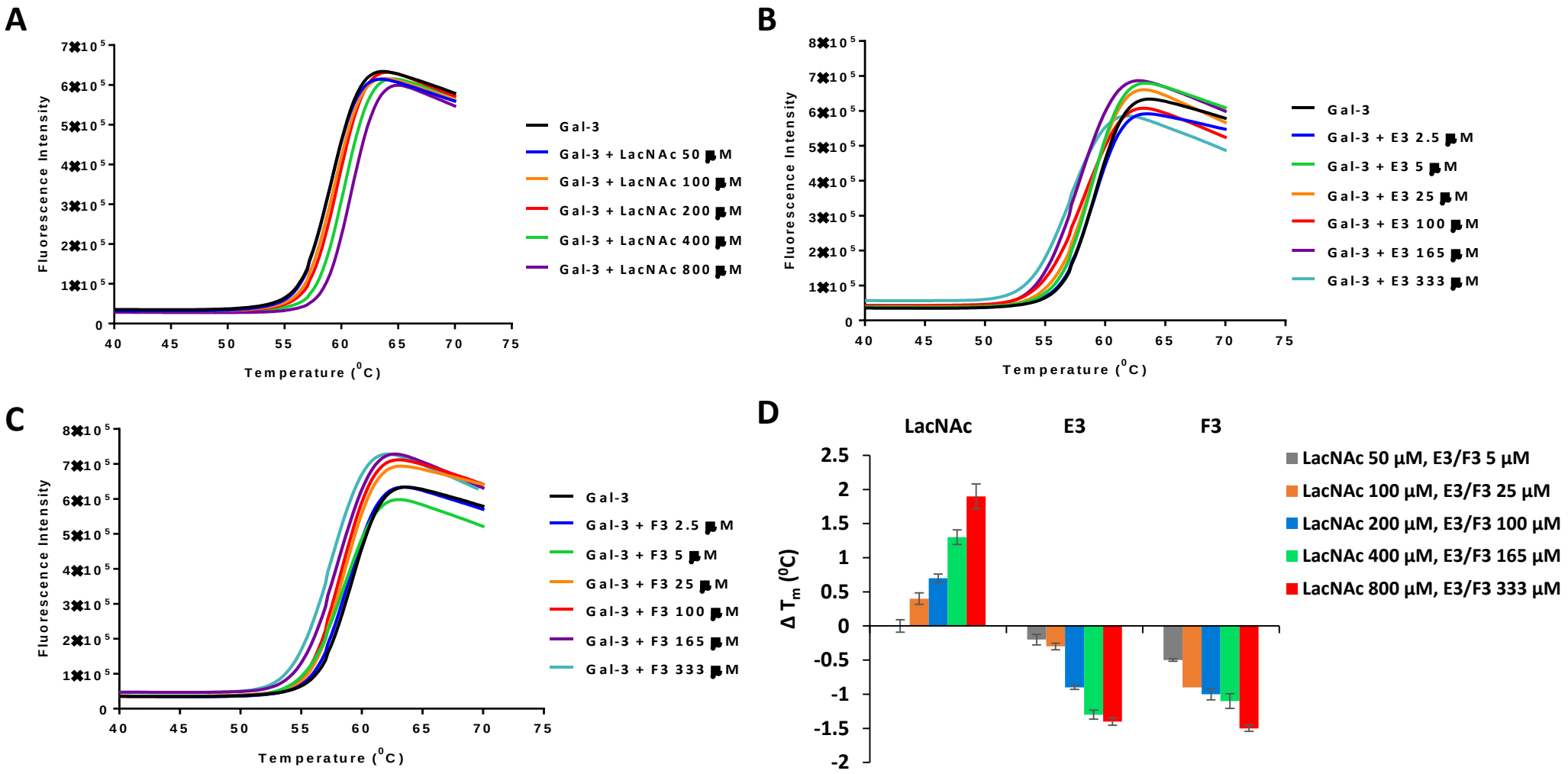
A
Fluorescence Intensity
Temperature (°C)
Gal-3
Gal-3 + LacNAc 50 μM
Gal-3 + LacNAc 100 μM
Gal-3 + LacNAc 200 μM
Gal-3 + LacNAc 400 μM
Gal-3 + LacNAc 800 μM
B
Fluorescence Intensity
Temperature (°C)
Gal-3
Gal-3 + E3 2.5 μM
Gal-3 + E3 5 μM
Gal-3 + E3 25 μM
Gal-3 + E3 100 μM
Gal-3 + E3 165 μM
Gal-3 + E3 333 μM
C
Fluorescence Intensity
Temperature (°C)
Gal-3
Gal-3 + F3 2.5 μM
Gal-3 + F3 5 μM
Gal-3 + F3 25 μM
Gal-3 + F3 100 μM
Gal-3 + F3 165 μM
Gal-3 + F3 333 μM
D
LacNAc
E3
F3
Δ Tm (°C)
LacNAc 50 μM, E3/F3 5 μM
LacNAc 100 μM, E3/F3 25 μM
LacNAc 200 μM, E3/F3 100 μM
LacNAc 400 μM, E3/F3 165 μM
LacNAc 800 μM, E3/F3 333 μM